# إزالةٌ فعَّالة لإمتزاز الصبغة الخضراء الفاقعة من المحاليل المائية بواسطة البنتونايت والبنتونايت المنشط حمضياً

# Effective Adsorptive Removal of Brilliant Green Dye from Aqueous Solution by Bentonite and Acid–activated Bentonite


د. محمد محمد حسن العواضي[1]

Dr. Mohammed Mohammed Al–Awadhi [2]



https://doi.org/10.54582/TSJ.2.2.20



(1) أستاذالكيمياء التحليلية المساعد بكلية التربية والعلوم– جامعة إقليم سبأ.

عنوان المراسلة : alawadhi2008@yahoo.com

(2) **Chemistry Department, Faculty of Education & Science, University of Saba Region, Marib, Yemen,**

**الملخص:**

في البحث الحالي، تم دراسة امتزاز الصبغة الخضراء الفاقعة (BG) من المحاليل المائية عن طريق تجارب الامتزاز الدفعي على البنتونايت اليمني (YB) والبنتونايت المنشط بالحمض (A-AYB). الدراسات المتعلقة بالعوامل المؤثرة على السعة الامتزازية لـ (YB) و( A-AYB) على سبيل المثال: الجرعة الممتزة، تركيز الصبغة الأولية، درجة الحموضة، القوة الأيونية، درجة الحرارة وزمن الاتزان دُرست ونُقشت بشكل منهجي. وأظهرت النتائج أن (YB) أظهرت قدرات امتزاز عالية نحو الأصباغ القاعدية في حين أظهرت (A-AYB) قدرات أمتزاز أقل من(YB). تم تحليل بيانات الحركية باستخدام نماذج نظام الرتبة الأول ونظام الرتبة الثانية. تم دراسة بيانات الايسوثيرم طبقا لمعادلات لانجمير Langmuir فريندليش Freundlich. تم حساب عوامل الديناميكية الحرارية $\Delta G°$، $\Delta H°$ و $\Delta S°$ لإمتزاز صبغة BG على YB و A-AYB؛ وأظهرت قيمة $\Delta G°$ الطبيعة التلقائية لامتزاز كل من المواد الماصة تحت الدراسة.

**الكلمات المفتاحية:** البنتونايت، الصبغة الخضراء الفاقعة; الامتزاز، الايسوثيرم، الديناميكية الحرارية

**Abstract**

In the present work, Adsorption of Brilliant Green (BG) from aqueous solutions via batch sorption experiments onto Yemen bentonite (YB) and Acid-activated bentonite (A-AYB) has been investigated. Studies concerning the factors influencing the adsorption capacities of YB and A-AYB for example: adsorbent dosage, initial dye concentration, pH, ionic strength, temperature and contact time were systematically studied and discussed. The results show that YB demonstrated high adsorption capacities toward basic dyes while A-AYB exhibited sorption capacities lower than YB. The kinetics data were analyzed using first order and pseudo-second order models. The isotherm data were investigated according to Langmuir and Freundlich equations. Thermodynamic parameters $\Delta G°$, $\Delta H°$ and $\Delta S°$ were calculated for the adsorption of BG on YB and A-AYB; the value of $\Delta G°$ showed the spontaneous nature of adsorption for both sorbents.

*Keywords:* bentonite; Brilliant green; Adsorption; Isotherm; Thermodynamic.

## Introduction

Dyes could be considered as one of the most serious pollutants, among which were released to the environment from industries [1]. Brilliant Green (BG) is frequently used in veterinary medicine, textile dying, and paper printing as a biological dye, dermatological agent, and a supplement to hens' feed to prevent the spread of mildew, intestinal parasites, and fungus. However, BG has adverse effects on humans and the environment. It causes irritation to the gastrointestinal tract and respiratory tract, symptoms include nausea, vomiting, and diarrhea. BG decomposition leads to generation of nitrogen oxides, carbon oxides, and sulfur oxides. Therefore, wastewater containing BG needs to be treated before its disposal in the environment [2-5]. There are various methods for dye removals, such as biological methods, oxidation-ozonation, and membrane filtration, coagulation, advanced oxidation, integrated treatment processes and adsorption [6-10]. The adsorption process is one of the simplest and most effective techniques with easy working conditions for many applications, such as wastewater treatment, liquid mixture separation and purification, or polar organic solute recovery from biotechnology processes [11,2]. Adsorption is a widely used technique for removing dyes because of its low cost, high efficiency, ease of usage, and environmental friendliness [12,1] [5, 6]. Bentonite is widely applied in many fields of adsorption technology as highly adsorbents because of their high specific surface area, sustainable, low-cost and effective adsorbents for the removal of BG from aqueous solution because of their profusion in nature and owning lasting negative charges and exchangeable cations[13].

Bentonite is a clay mineral, which is mainly composed of montmorillonite with chemical composition of $SiO_2$, $Al_2O_3$, $Fe_2O_3$,


https://doi.org/10.54582/TSJ.2.2.20

CaO, MgO, $K_2O$, $Na_2O$. It includes of one octahedral alumina sheet lying between two tetrahedral layers of silica [14]. The isomorphous replacement of $Mg^{2+}$ for $Al^{3+}$ in the octahedral layer and $Al^{3+}$ for $Si^{4+}$ in the tetrahedral layer is responsible for bentonite's permanent negative charge. The presence of replaceable cations ($Na^+$, $Ca^{2+}$, etc.) in the lattice structure balances this negative charge, enhancing the adsorption of cationic pollutants [15-17].

Yemen Bentonite was used for this study because of its local profusion and contain a high percentage of the active components which may make it of potential industrial applications[18]. Although it is probable to increase the physicochemical activity and surface area of YB by acid activation, the relationship between the structural change and adsorption kinetics of YB is not obvious after acidification via mineral acid [19]. So, it is very significant to study the adsorption of organic cations on YB and A-AYB. The aim of this study was to test the adsorption behavior of large organic cation from aqueous solution on YB and A-AYB. It may be useful to environmental engineers for designing and establishing a continuous treatment plant for wastewaters and water by using the data obtained. To explain the character of the YB surface in the BG adsorption process, the effects of initial BG concentration, temperature, and contact time were investigated.

## 1. Experimental

### 1.1. Materials

Bentonite applied in this study was obtained from Yemen with chemical component of 70.28% $SiO_2$, 13.23% $Al_2O_3$, 7.25 $Fe_2O_3$, 1.38% $Na_2O$, 0.11% MgO, 0.21% CaO and 1.18% $TiO_2$, 1.87% $K_2O$, 4.6% Loss of ignition (determined by x-ray fluorescence).

Without any additional purification, BG was used. A stock solution of 1000 mg/L was prepared by dissolving a weighed amount of BG in 1000 mL of distilled water. When needed, the experimental solution was prepared via diluting the stock solution with distilled water. The BG structure of this dye is illustrated in Fig. 1.

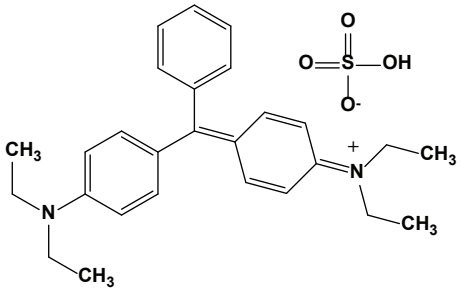


**Fig. 1**: The chemical structure of Brilliant Green dye.

### 1.2. Synthesis of acid-activated bentonite (A-AYB)

The acid-activated bentonite was synthesized by the following steps. For A-AYB preparation, 25 mL of 3 N HCl were added slowly to 15 g sample of the dried YB for 4 hr. at the boiling point (~ 378 K) with continuous stirring. After that, the product was filtered and washed recurrently with bi-distilled water until no $Cl^-$ ion was detected by $CH_3COOAg$ solution (0.1M). The A-AYB was dried at 110 °C for 8 hr.

### 1.3. Characterization

Surface area of the YB and A-AYB was estimated by BET method (Brunauer–Emmet–Teller) using liquid $N_2$ adsorption at 77 °K by means of a conventional volumetric apparatus. This was determined by a McLeod system connected to the apparatus.

The morphology of the samples surfaces were studied using


https://doi.org/10.54582/TSJ.2.2.20

scanning electron microscopy (SEM, model JSM-T 220A, JEOL, Japan) at an accelerated voltage 20 KV.

FTIR spectra were analyzed via a Nicolet FTIR spectrophotometer using KBr in a wavenumber range of 4000–400 $cm^{-1}$ with a resolution accuracy of 4 $cm^{-1}$.

### 1.4. Adsorption studies

The batch sorption was effected on Shaking Water Bath (NE5, Nickel-Electro Ltd.,UK) at 240 rpm. To study the effect of YB and A-AYB on sorption capacities of BG experiments, 0.1 g adsorbent and 50 mL BG solution (initial conc.1000 $mgL^{-1}$, natural pH 6.95) were used. The system was operated under shaking at 25 °C till adsorption balance was reached. The influence of pH on BG removal was investigated by adjusting 50 ml BG solutions (1000 mg/L) at pH (2.0-10.0) using 0.01 mol/L HCl or NaOH solution with 0.1 g adsorbent for 90 min at 25°C. The influence of temperature on BG elimination was tested in the 50 mL BG solutions (1000 $mgL^{-1}$, pH 7) by adding 0.1g adsorbent till balance was completed. The effect of sorption time on BG removal was effected in the 50 ml BG solutions (700 $mgL^{-1}$, pH 7) by adding 0.1 g adsorbent at 25 °C for determined period of time. The effect of the initial BG concentration on BG removal was tested by exciting 50 mL with several dye concentrations of BG solution at conditions: 0.1 g/50 mL; pH 7; T 25°C; 120 min. Afterward, the samples were filtered and the adsorbate of residual concentrations was measured. The quantities of BG removed by sorbents $q_e$ and percent extracted %E can be calculated by the following equations:

$$q_e = \frac{(C_o - C_e)V}{m} \qquad (1)$$

$$\% E = \frac{(C_\circ - C_e)}{C_\circ} \times 100 \qquad (2)$$

Where $q_e$ (mg/g) is the equilibrium concentration of BG on the adsorbent, the initial and equilibrium dye liquid-phase concentrations (mg/g) are $C_0$ and $C_e$, respectively, m (g) is the mass of the adsorbent and V (L) is the volume of solution. The concentration of BG in the residual solution was analyzed spectrophotometrically by UV-Vis spectrophotometer at wavelength 623 nm and the amount of adsorption $q_t$ was calculated according to equation (1).

## 2. Result and discussion

### *1.1* Characterization of YB and A-AYB

The surface area and porosity of an adsorbent are important parameters in determining its adsorption capacity as well as its adsorption performance [20]. The acidification can be replacement of exchangeable cations ($Na^+$, $Ca^{2+}$, $K^+$) with $H^+$ ions, eliminate impurities, and leaching of $Fe^{3+}$, $Al^{3+}$ and $Mg^{2+}$ from the tetrahedral and octahedral sites in YB which exposes the edges of platelets[21].

**Table 1**: The textural properties of the investigated YB and A-AYB as determined from nitrogen adsorption isotherms

| Adsorbent | YB | A-AYB |
|---|---|---|
| Surface area $S_{BET}$ ($m^2/g$) | 79.024 | 170.379 |
| BET-C constant | 30.65 | 213.25 |
| Pore volume $V_T$ (ml/g) | 0.01624 | 0.0662 |
| Average pore diameter. r (nm) | 0.411 | 0.777 |

These textural activations are illustrated when the textural properties of YB are compared with those of A-AYB. The evident changes in the textural parameters caused by activated YB by HCl may


https://doi.org/10.54582/TSJ.2.2.20

be ascribed to the construction of smaller pores takes place as the impurities are removed and the exchangeable cations are substituted by $H^+$ ions[22]. To obtain evidence for the adsorption of Acid-activated and BG into YB sample, the FTIR spectra of YB, A-AYB and Brilliant Green loaded YB (BG-YB) are showed in Fig. 2(a, b, c) and table 2. The broad absorption bands observed at 3360–3640 $cm^{-1}$ are caused by the O–H stretching vibration of the Si–OH bands and HO–H vibration of the $H_2O$ adsorbed silica surface and a band appear at 1630 $cm^{-1}$ is due to the $H_2O$ bending vibration [23]. The broad bands at 1090-1035 $cm^{-1}$ are related to the stretch vibrations of Si-O in the Si-O-Si groups of the tetrahedral sheet, also the bands at 525 and 468 $cm^{-1}$ are caused by Si-O-Al (octahedral sheet) and Si-O-Si bending vibrations[24]. For BG-YB, two peaks appear at 3018, 2915 $cm^{-1}$ which represent the stretching vibration of -CH- aromatic and $-CH_3$ methyl groups of BG, the band near 1632 $cm^{-1}$ is related to the N=C, and the peaks at 1412-1340 $cm^{-1}$ area and the feature compatible to the C=C skeleton stretching at 1590 $cm^{-1}$ produce from the aromatic ring vibrations of BG (Fig. 2c). The band of amorphous silica was shown in the range of 1260-1130 $cm^{-1}$ (Fig. 2b) [19]¼đ . Activated of YB by HCl was associated also with apparent change in the morphology and particle size.

The SEM images of YB and A-AYB are shown in Figs. 3a and 3b, respectively. Evidently, the agglomerates of YB contain few numbers of particles compared with those A-AYB. The particles of A-AYB are more eroded than the particles of YB which increased the surface area. This acidification modify the morphology of the YB as the pores open up, so the SEM images of YB and A-AYB confirms the results obtained from surface area.

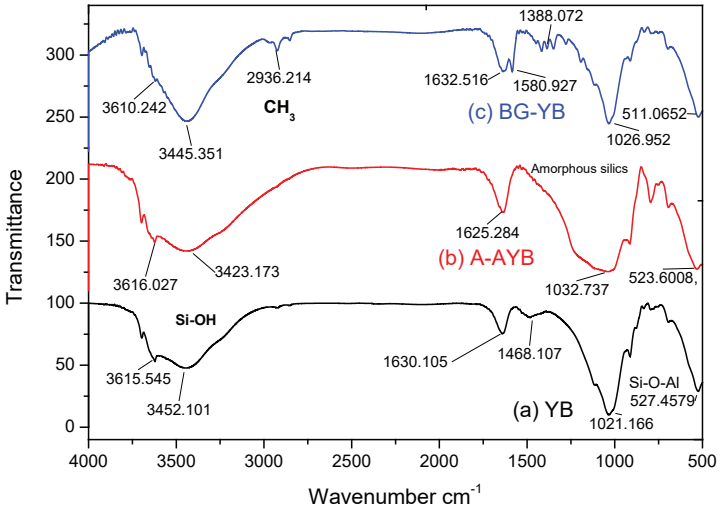


**Figs. 2**: FTIR spectra of (a) YB, (b) A-AYB and (c) BG-YB

**Table 2**: FTIR spectra data of YB, A-AYB and BG-YB.

| Assignment | YB $cm^{-1}$ | A-AYB $cm^{-1}$ | BG-YB $cm^{-1}$ |
|---|---|---|---|
| Si-OH bands and H-O-H stretching | 3615<br>3452 | 3616<br>3423 | 3610<br>3445 |
| CH- aromaic and- $-CH_3$ stretching | - | - | 3018<br>2915 |
| H-O-H bending | 1630 | 1625 | 1632 |
| N=C<br>C=C stretching | - | - | 1632<br>1590 |
| amorphous silica | | 1260-1130 | |
| Si-O-Si stretching | 1021 | 1032 | 1026 |
| Si-O-Al bending | 527 | 523 | 511 |


https://doi.org/10.54582/TSJ.2.2.20

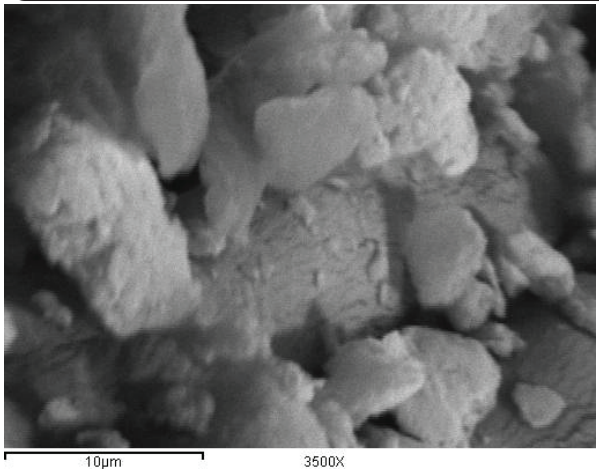


**Figs**. **3a**: SEM micrographs of YB

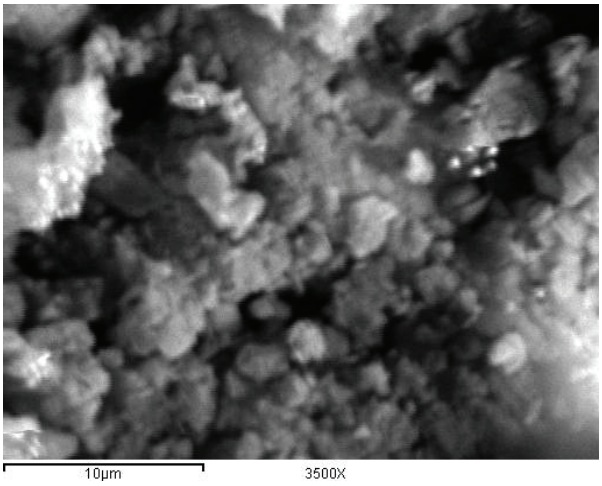


**Figs**.**3b**: SEM micrographs of A-AYB

## *1.2* Effect of pH on BG adsorption

The pH of the solution, which influences the adsorbent's surface charge and the adsorbate's speciation, was a key regulating parameter in the adsorption process. The effect of pH on BG onto YB and A-AYB elimination from aqueous solution is shown in Fig. 4. The adsorption capacity increased dramatically from 258.4

to 395.4 mg/g and from 98.4 to 197.6 for YB and A-AYB respectively, when the pH of the dye solution was increased from 2 to 10. The attraction between cationic dye molecules BG and abundant $HO^-$ ions at alkaline pH levels may be responsible for the substantial increase in adsorption. BG sorption onto modified mesoporous clay[25] and vegetal fiber activated carbons[26] and vegetal fiber activated carbons has also been shown to have similar results.

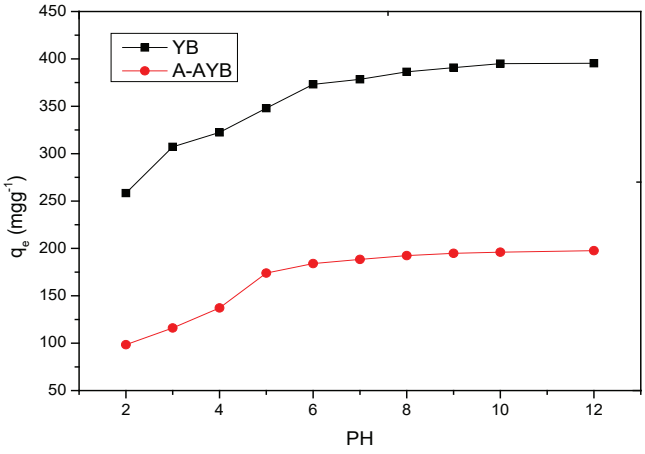


**Fig. 4**: Effect of the pH values on adsorption capacity of BG by YB ■ and A-AYB ● (Conditions: $C_o$ = 800 mg/L; adsorbent dose = 0.1 g/50 mL; T=25°C; equilibrium time, 160 min).


https://doi.org/10.54582/TSJ.2.2.20

### *1.3* Effect of Concentration

In general, dye sorption was dependent on the dye's initial concentration [27]. The effect of initial BG concentration on the adsorption capacity of YB and A-AYB towards BG is shown in Fig. 5. It can be shown that $q_e$ increased sharply from 346.88 to 378.4 mg/g with increasing the initial BG concentration from 700 to 800 mg/l while that of A-AYB was 186.4 mg/g to196.6 mg/g from 400 to 500 mg/l. However, the amount of BG adsorbed at equilibrium ($q_e$) enhanced slightly from 378.4 to 390 mg/g with an increase in the initial BG concentration from 800 to 1200 mg/l while that of A-AYB was 196.6 mg/g to203.6 mg/g from 500 to 1200 mg/l at 25 °C. Fig.5 shows higher elimination of BG onto YB than that of A-AYB. An increase in adsorbate concentration appears to cause an increase in driving force, which then in turn gives rise in the BG rate of diffusion [28]. The amount of BG adsorbed at equilibrium ($q_e$) increase from 50 to 390.01 mg/g and from 49.792 to 203.06 mg/g, for YB and A-AYB respectively, indicating that YB is an efficient adsorbent for BG.

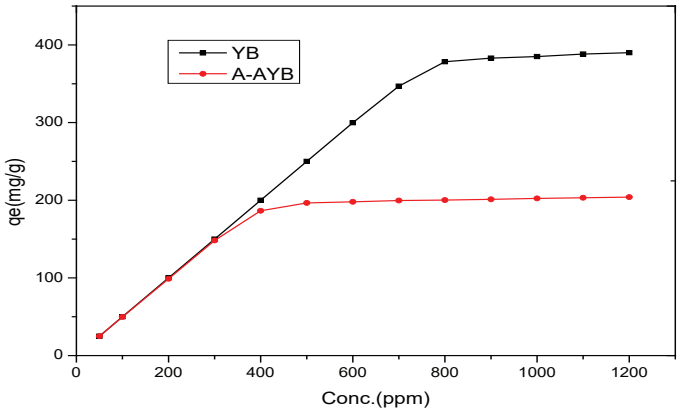

**Fig. 5**: Effect of of initial dye concentration on adsorption capacity of YB ■ and A-AYB ● for BG. (Conditions: adsorbent dose = 0.1 g/50 mL; T=25°C; equilibrium time, 180 min).

## *1.4* Effect of amount of adsorbent

The effect of adsorbent dosage on removal of BG by Bentonite and A-AYB is shown in Fig. 6. When the sorbent dose increases from 0.025 to 0.2 g, the percent dye removals by YB and A-AYB increase from 27.51 % to 99.97 % and from 8.61 % to 84.43 %, respectively. The adsorption of the BG increased significantly as the dose of adsorbent increased from 0.025 to 0.075 g, and increased slightly from 0.1 to 0.25 g. This can be simply attributed to the increased sorbent surface area and the availability of more sorption sites. However, because of the high number of unsaturated adsorption sites, the amount of BG adsorbed (mg/g) was shown to decrease as the adsorbent dosage was increased.

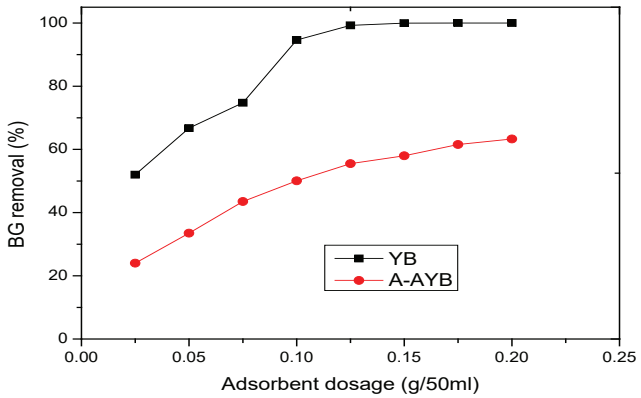


**Fig. 6**: The effect of adsorbent dosage YB and A-AYB on BG removal. (Cond.: $C_o$ = 800 mg/L; T=25°C; equilibrium time, 24 h).


https://doi.org/10.54582/TSJ.2.2.20

### *1.5* Effect of volume of Brilliant Green.

BG solution volume is one of the factors that influences the effective capacity of the adsorption for BG. Various BG volumes (0.025-0.25L) with 0.1g sorbent were applied at pH 6.9, 25 $^0$C, and BG 600 mg/l. Fig. 7 show higher removal of BG onto YB than that of A-AYB. BG removal decreased slightly from 99.99% to 57.30% (YB) and from 74.53% to 21.35% (A-AYB) with increasing BG volume from 0.025 to 0.25 L.

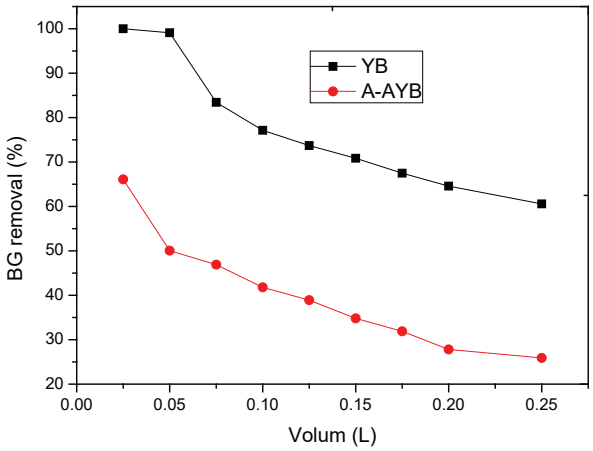


**Fig**. **7**: The effect of volume BG on YB and A-AYB. (Conditions: $C_o$ = 800 mg/l; .(T=25°C; equilibrium time, 24 h

### *1.6* Effect of contact time on adsorption

Fig. 8 shows the effect of contact time on YB and A-AYB sorption capacity in BG dye solution at 700 ppm concentration. The sorption capacity of YB and A-AYB increases rapidly as the contact time is increased from 0 to 90 minutes, with more than 92 percent

of the equilibrium sorption capacity for BG obtained at 90 minutes. After 120 min, the sorption capacity became constant and the adsorption equilibrium accomplished. Consequently, 120 min was chosen as the contact time for the sorption of BG onto the aggregates under our study conditions. As shown, the sorption process was divided into three steps: (a) an initial step with sorption occurring promptly, (b) subsequently slow sorption, and (c) a final step with sorption getting equilibrium and residual constant. The first step can be attributed to the rapid attachment of BG to the surface of the bentonites by surface mass transfer. At this step (0-20 min), more than 85% of BG adsorption was achieved in YB, while more than 55% was achieved in A-AYB. The second step was slower (20-90), probably because many of the available external sites was already occupied and due to the slow diffusion of BG molecules into the network of bentonites. The kinetics of the sorption process shows that the adsorption of BG onto YB and A-AYB indicate a fast sorption process because more than 85 % of BG was adsorbed within 20 min especially at BG concentration lower than the maximum adsorbed. This result exposes the advantages of using this low-cost adsorbent, for the treatment of aqueous solutions loaded in dyes in overall and BG in specifically.

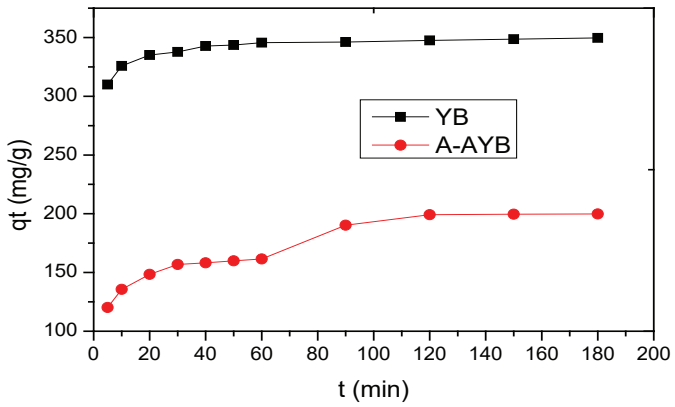



https://doi.org/10.54582/TSJ.2.2.20

**Fig**. **8**: Effect of contact time on the adsorption capacity of YB and A-AYB for BG. (Conditions: dose = 0.1 g/50 mL; T=25°C; $C_o$ = 700 mg/l).

## *1.7* Effect of ionic strength

The availability of salt in water leads to high ionic strength may be more effective on the efficiency of the adsorption process [13]. As can be shown in Fig. 9, the variation of salts concentration (NaCl, KCl, and $CaCl_2$) makes a major effect on the range of basic dyes adsorption. The current study indicates that the sorption of positively charged BG, on negatively charged YB and positively charged A-AYB decreased with the addition of in the order: NaCl< KCl < $CaCl_2$. The increase of ionic strength in aqueous solution may result in the compression of the diffuse double layer on the adsorbent, which eases the electrostatic attraction and contributes to the adsorption consequently [29].

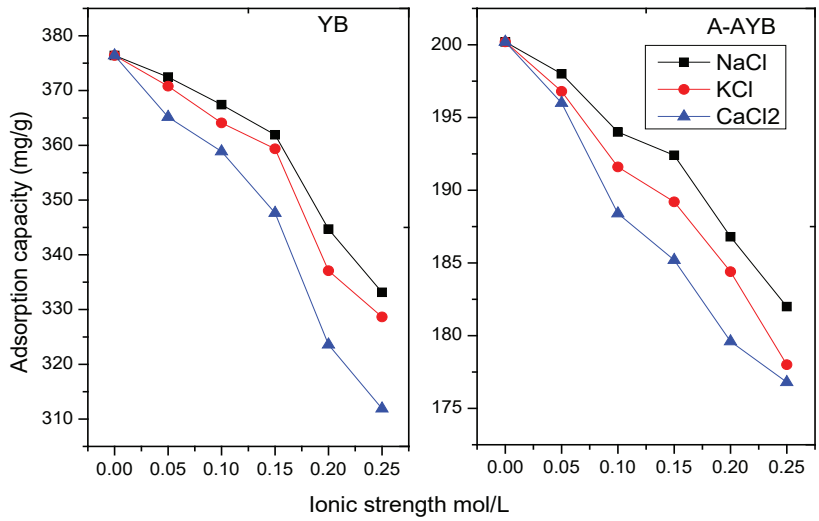


**Fig**. **9**: Effect of ionic strength on the removal of BG by YB and A-AYB (Condi-


المجلد(3) العدد(2) مايو 2022م
https://doi.org/10.54582/TSJ.2.2.20

tions: $C_o$ = 800 mg/l; time = 6 h; adsorbent dose = 0.1 g/50 ml; T=25° C).

### *1.8* Effect of temperature on adsorption

The effect of temperature on adsorption was studied at 25, 35and 45°C, and the consequences are shown in Table 3. It could be obviously seen that the amount adsorbed at equilibrium increases with increasing temperature. When the temperature increased from 25 °C to 45 °C, the maximum amounts of BG removed by YB and A-AYB are found to be increased from 336.742 to 352.472 mg/g and 172.58 to 178.99 mg/g respectively. It is found that higher temperature eased the sorption of BG on YB. Increased temperature is known to cause swelling inside the adsorbent structure, penetrating the additional large dye molecule, and this effect can be attributed to the enlargement of pores and the creation of new active sites on the adsorbent surface due to bond distortion with increasing temperature[30].

**Table 3**: Effect of temperature on maximum adsorption capacities of BG by YB A-AYB.

| Samples | $q_e$ (mg $g^{-1}$) | | |
|---|---|---|---|
| | 25 °C | 35°C | 45°C |
| YB | 378.4 | 379.84 | 381.6 |
| A-AYB | 186.4 | 187.6 | 188.08 |

### Adsorption kinetics

The value constant of adsorption is specified from the first-order kinetic rate expression given by Lagergren [31] can be expressed as Eq. (3):

$$\log(q_e - q_t) = \log q_e - \frac{K_1 t}{2.303} \qquad (3)$$

Where $q_e$ and $q_t$ (mg/g) are the amounts of BG adsorbed at equilib-


https://doi.org/10.54582/TSJ.2.2.20

rium and at time t, respectively and k, is the equilibrium constant ($min^{-1}$) which were obtained from the slopes of the linear plots of $\ln(q_e - q_t)$ versus time Fig. (10a).

The kinetics of pseudo-second-order model is depended on the supposition of chemisorption of the adsorbate onto the adsorbents. This model[32] can be expressed as Eq. (4):

$$\frac{t}{q_t} = \frac{1}{K_2\, q_e^2} + \frac{t}{q_e} \quad (4)$$

Where $K_2$ (g/mg min) is the equilibrium rate constant for the pseudo second-order kinetic adsorption and $q_e$ can be computed from the plot of $t/q_t$ against t Fig. (10b). A comparison of the results with the correlation coefficients for the first-order kinetic and second-order kinetic models is shown in Table 4. For YB and A-AYB: the second order model is the best fit model for experimental kinetic data this because of the value of the calculated $q_e$ agree very well with the experimental data and $r^2$ is greater than 0.98 for all adsorbents. These results also indicated that the applicability of this kinetic equation and the second-order nature of the adsorption process of BG on clays [33].

**Table 4**: Kinetic parameters for the adsorption of BG onto YB and A-AYB.

| | Pseudo first-order kinetic model | | | |
|---|---|---|---|---|
| | $q_{e,exp.}$ (mg $g^{-1}$) | $q_{e,1cal}$ (mg $g^{-1}$) | $k_1$ ($min^{-1}$) | $R_1^2$ |
| **YB**: | 349.64 | 27.121 | 0.022 | 0.9874 |
| **A-AYB**: | 199.61 | 94.06 | 0.0259 | 0.985 |


https://doi.org/10.54582/TSJ.2.2.20

| | Pseudo second-order kinetic model | | | |
|---|---|---|---|---|
| | $q_{e,exp.}$ (mg $g^{-1}$) | $q_{e,2\ cal}$ (mg $g^{-1}$) | $k_2$ (g $mg^{-1}$ $min^{-1}$) | $R_2^2$ |
| **YB**: | 349.64 | 337.838 | $-8.698*10^{-9}$ | 0.99863 |
| **A-AYB**: | 199.612 | 264.55 | $5.127*10^{-7}$ | 0.9868 |

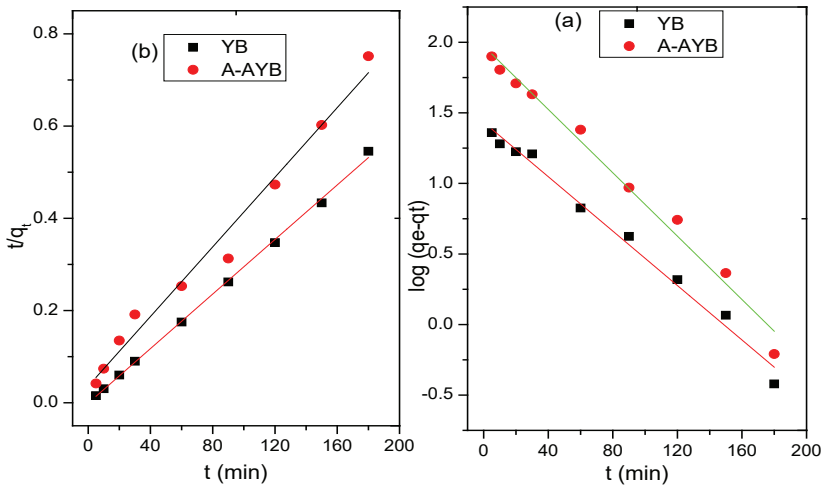


**Fig.10**: (a) Pseudo-first-order kinetic and (b) Pseudo-second-order kinetic model for the adsorption of BG by YB and A-AYB at initial concentrations 700 ppm.

## *1.9* Adsorption isotherms

The Langmuir and Freundlich isotherm equations were used to explain the equilibrium adsorption isotherms, which are defined by the following equations:

$$\frac{C_e}{q_e} = \frac{1}{bq_m} + \frac{C_e}{q_m} \qquad (5)$$

$$q_e = K_f C_e^{\frac{1}{n}} \qquad (6)$$

where b is Langmuir equilibrium constant ($L.mg^{-1}$), and $q_m$ ($mg.g^{-1}$) is the monolayer adsorption capacity; $K_f$ ($mg.g^{-1}$) and n are the Freundlich constants.The Freundlich parameters can be obtained by the following linearized equation:

By linearly plotting ln $q_e$ as the function of ln Ce, the values of $K_f$ and n can be obtained from the intercept and the slope of the plot (Fig. 11).The isotherm parameters for the adsorption of BG onto YB and A-AYB are given in Table 5. Langmuir adsorption model provides the best fit with experimentally obtained data for YB and A-AYB with ($r^2$ = 0.9999). However the Freundlich adsorption can be used also for modeling the equilibrium data for YB and A-AYB ($r^2$ = 0.895, 0.954). This shows the surface of YB was enveloped by the monolayer of BG. The adsorption capacities for BG onto YB and A-AYB are in good agreement with the previously reported data in Table 6.

**Table 5**: Adsorption isotherm parameters for the adsorption of BG on YB and A-AYB

| **Adsorbent** | | **YB** | **A-AYB** |
|---|---|---|---|
| **Langmuir** | $q_{max}$ (mg/g) | 389.105 | 201.207 |
| | b (L/mg) | 2.073 | 0.542 |
| | $R^2$ | 0.99995 | 0.99997 |
| **Freundlich** | $K_f$ (mg/g) | 334.856 | 173.296 |
| | n | 37.9363 | 40.8831 |
| | $R^2$ | 0.89489 | 0.95408 |

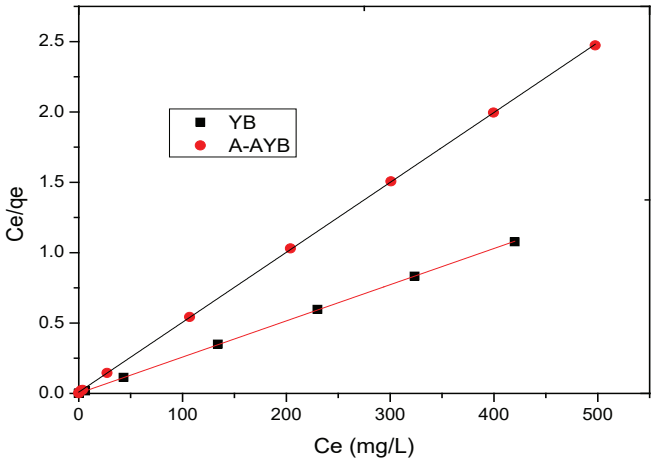


**Fig. 11**: Langmuir plot for the adsorption of BG by YB and A-AYB at 25 °C

**Table 6**: Comparison of adsorption capacities of various adsorbents for BG.

| Adsorbents | Adsorption capacity (mg/g) | Reference |
|---|---|---|
| YB | 389.105 | Present study |
| A-AYB | 201.207 | Present study |
| activated carbon from medlar nucleus | 833.15 | [34] |
| activated carbon from date pits | 311.38 | [35] |
| polyurethane foam with coal | 134.95 | [36] |
| red clay | 125 | [33] |
| kaolinite clay mineral | 50.51 | [37] |
| cotton shell powder | 252.17 | [38] |
| Poly(AN-co-VP)/Zeolite | 23.81 | [39] |

### *1.10* Thermodynamic study

Thermodynamic parameters were computed from the difference of the thermodynamic distribution coefficient, Kc with change in temperature. The standard free energy change, ΔG°, was calculated using the expression:

$\Delta G° = -RT \ln Kc$ (7)

$\Delta G° = \Delta H° - T\Delta S°$ (8)

where R is gas constant (8.314 J/mol/K), T the absolute is temperature in $K^0$ and $K_c$ is the Langmuir constant. Standard enthalpy ($\Delta H^o$) and entropy ($\Delta S^o$) of adsorption could be estimated from Van't Hoff equation[40] :

$$\ln k_c = \frac{\Delta S}{R} - \frac{\Delta H}{RT} \quad (9)$$

By plotting a graph of lnKc versus 1/T (fig. 12), the values of ΔH° and ΔS° can be estimated from the slope and intercept of van't Hoff plots, respectively. The thermodynamic parameters are offered in Table 7. It is evident from the table that the values of ΔG° are negative for YB and A-AYB. The negative values of ΔG°for all adsorbents at various temperatures indicate the process to be feasible and spontaneous. Actually, the fact that the values of the ΔG° decrease with increasing temperature shows the increase of spontaneous influence. For all the sorbents, the positive value of ΔH° suggested the endothermic nature of the adsorption process. Moreover, the positive value of ΔS° also indicates the increased randomness during sorption process.

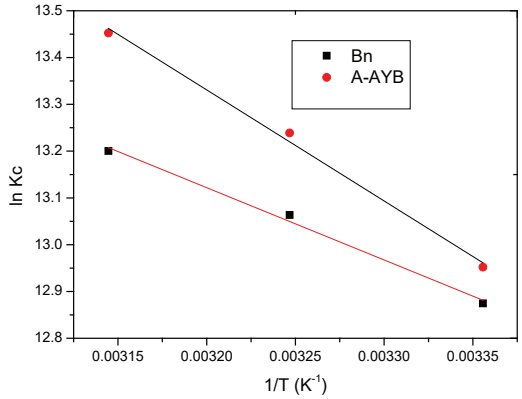


**Fig.12**: The plots of lnKc versus 1/T for estimations of thermodynamic parameters of the adsorption process.

**Table 7**: Thermodynamic parameters for adsorption of BG by YB and A-AYB at different temperatures.

| Sample Code | ΔH° (KJ/mol) | ΔS° (KJ/molK) | ΔG° (KJ/mol) | | |
|---|---|---|---|---|---|
| | | | 298 K | 308 K | 318 K |
| YB | 12.8458 | 0.15020 | -31.8979 | -33.4519 | -34.8993 |
| A-AYB | 19.7363 | 0.173989 | -32.0897 | -33.9008 | -35.5663 |

## 1.1 Conclusion

In the present study, YB clay was selected as a local, cheap and readily available adsorbent application in the treatment of industrial wastewater and water polluted with dyes. YB and A-AYB were characterized using nitrogen adsorption isotherms, FTIR and SEM. Adsorption of the BG dye was studied by batch adsorption experiments. FTIR and SEM analyses confirmed modification of Yemen YB treated by acid. The amount of BG adsorbed was found to increase in order YB (389.105 mg/g >A-AYB (201.207 mg/g). The results revealed that the adsorption of the dye increases with increasing the pH using YB and A-AYB. In addition, they indicated a gradual increase in the percentage removal of BG dye with temperature for YB and A-AYB. An optimum dosage of both YB and A-AYB is 2 $gL^{-1}$. The adsorption kinetic studies showed that the elimination of BG is a rapid process and the adsorption process obeys the pseudo-second order model, indicating that cationic dye has a very strong affinity for the YB surface. The Langmuir model agrees with experimental data well. Thermodynamic studies showed that the adsorption process was endothermic and spontaneous in nature. Through the positive results obtained from this study in the removal of cationic organic compounds, we recommend that wastewater treatment engineers use YB in treatment plants to remove cationic organic compounds.

## 3. References

1. Kismir Y, Aroguz AZ (2011) Adsorption characteristics of the hazardous dye Brilliant Green on Saklıkent mud. Chemical Engineering Journal 172 (1):199-206

2. Singh K, Gupta A, Sharma A (2016) Fly ash as low cost adsorbent for treatment of effluent of handmade paper industry-Kinetic and modelling studies for direct black dye. Journal of Cleaner Production 112 (1):1227-1240

3. Mane VS, Babu PV (2011) Studies on the adsorption of Brilliant Green dye from aqueous solution onto low-cost NaOH treated saw dust. Desalination 273 (2-3):321-329

4. Kumar R, Barakat M (2013) Decolourization of hazardous brilliant green from aqueous solution using binary oxidized cactus fruit peel. Chemical engineering journal 226 (1):377-383

5. Bhattacharyya KG, Sarma A (2003) Adsorption characteristics of the dye, Brilliant Green, on Neem leaf powder. Dyes and pigments 57 (3):211-222

6. Javaid M, Saleemi AR, Naveed S, Zafar M, Ramzan N (2011) Anaerobic treatment of desizing effluent in a mesophilic anaerobic packed bed reactor. Journal of the Pakistan Institute of Chemical Engineers 39 (1):61-67

7. Qian F, Sun X, Liu Y (2013) Removal characteristics of organics in bio-treated textile wastewater reclamation by a stepwise coagulation and intermediate GAC/O3 oxidation process. Chemical Engineering Journal 214 (1):112-118

8. Kurt E, Koseoglu-Imer DY, Dizge N, Chellam S, Koyuncu I (2012) Pilot-scale evaluation of nanofiltration and reverse osmosis for process reuse of segregated textile dyewash wastewater. Desalination 302 (1):24-32

9. Aziz F, Rehman MS, Batool A, Muhammad A, Mahmood T (2012) Pretreatment of municipal, industrial and composite wastewater by ozonation. Environ Process Eng 1 (1):1-8

10. Lotito AM, Fratino U, Bergna G, Di Iaconi C (2012) Integrated biological and ozone treatment of printing textile wastewater. Chemical Engineering Journal 195 (1):261-269

11. Rehman MSU, Kim I, Han J-I (2012) Adsorption of methylene blue dye from aqueous solution by sugar extracted spent rice biomass. Carbohydrate polymers 90 (3):1314-1322

12. Ghaedi M, Negintaji G, Marahel F (2014) Solid phase extraction and removal of brilliant green dye on zinc oxide nanoparticles loaded on activated carbon: new kinetic model and thermodynamic evaluation. Journal of Industrial and Engineering Chemistry 20 (4):1444-1452

13. Liu Y, Kang Y, Mu B, Wang A (2014) Attapulgite/bentonite interactions for methylene blue adsorption characteristics from aqueous solution. Chemical Engineering Journal 237 (1):403-410

14. Li Q, Yue Q-Y, Sun H-J, Su Y, Gao B-Y (2010) A comparative study on the properties, mechanisms and process designs for the adsorption of non-ionic or anionic dyes onto cationic-polymer/bentonite. Journal of Environmental Management 91 (7):1601-1611

15. Tahir S, Rauf N (2006) Removal of a cationic dye from aqueous solutions by adsorption onto bentonite clay. Chemosphere 63 (11):1842-1848

16. Wang C-C, Juang L-C, Hsu T-C, Lee C-K, Lee J-F, Huang F-C (2004) Adsorption of basic dyes onto montmorillonite. Journal of colloid and interface science 273 (1):80-86

17. Ishaq M, Sultan S, Ahmad I, Saeed K (2017) Removal of Brilliant Green Dye from Aqueous Medium by Untreated Acid treated and Magnetite Impregnated Bentonite Adsorbents. Journal of the Chemical Society of Pakistan 39 (5):780-787

18. Ismail R, Almaqtri W, Hassan M (2021) Kaolin and bentonite catalysts efficiencies for the debutylation of 2-tert-butylphenol. Chemistry International 7 (1):21-29

19. Hajjaji M, El Arfaoui H (2009) Adsorption of methylene blue and zinc ions on raw and acid-activated bentonite from Morocco. Applied Clay Science 46 (4):418-421

20. Yener N, Bicer C, Önal M, Sarıkaya Y (2012) Simultaneous determination of cation exchange capacity and surface area of acid activated bentonite powders by methylene blue sorption. Applied Surface Science 258 (7):2534-2539

21. Alshameri A, R Abood A, Yan C, Muhammad AM (2014) Characteristics, modification and environmental application of Yemen's natural bentonite. Arabian Journal of Geosciences 7 (3):841-853

22. Saha P, Chowdhury S, Gupta S, Kumar I (2010) Insight into adsorption equilibrium, kinetics and thermodynamics of Malachite Green onto clayey soil of Indian origin. Chemical Engineering Journal 165 (3):874-882

23. Shamsudin MS, Azha SF, Shahadat M, Ismail S (2019) Cellulose/bentonite-zeolite composite adsorbent material coating for treatment of N-based antiseptic cationic dye from water. Journal of Water Process Engineering 29 (1):755-764

24. Koswojo R, Utomo RP, Ju Y-H, Ayucitra A, Soetaredjo FE, Sunarso J, Ismadji S (2010) Acid Green 25 removal from wastewater by organo-bentonite from Pacitan. Applied clay science 48 (1-2):81-86

25. Hong S, Wen C, He J, Gan F, Ho Y-S (2009) Adsorption thermodynamics of methylene blue onto bentonite. Journal of hazardous materials 167 (1-3):630-633

26. Maia LS, da Silva AI, Carneiro ES, Monticelli FM, Pinhati FR, Mulinari DR (2021) Activated carbon from palm fibres used as an adsorbent for methylene blue removal. Journal of Polymers and the Environment 29 (4):1162-1175

27. Yeow PK, Wong SW, Hadibarata T (2021) Removal of azo and anthraquinone dye by plant biomass as adsorbent—a review. Biointerface Research in Applied Chemistry 11 (1):8218-8232

28. Garamon S (2019) Sequestration of hazardous Brilliant Green dye from aqueous solution using low-cost agro-wastes: Activated carbon prepared from rice and barley husks. Research on Crops 20 (4):886-891

29. ALzaydien AS (2009) Adsorption of methylene blue from aqueous solution onto a low-cost natural Jordanian Tripoli. American Journal of Applied Sciences 6 (6):1047

30. Ullah R, Iftikhar FJ, Ajmal M, Shah A, Akhter MS, Ullah H, Waseem A (2020) Modified clays as an efficient adsorbent for brilliant green, ethyl violet and allura red dyes: Kinetic and thermodynamic studies. Pol J Environ Stud 29 (5):3831-3839

31. Lagergren S (1898) About the theory of so-called adsorption of soluble substances. Kungliga Svenska Vetenskapsakademiens Handlingar 24 (4):1-39

32. Naghizadeh A, Kamranifar M, Yari AR, Mohammadi MJ (2017) Equilibrium and kinetics study of reactive dyes removal from aqueous solutions by bentonite nanoparticles. Desalination and Water Treatment 97 (1):329-377

33. Rehman MSU, Munir M, Ashfaq M, Rashid N, Nazar MF, Danish M, Han J-I (2013) Adsorption of Brilliant Green dye from aqueous solution onto red clay. Chemical engineering journal 228 (1):54-62

34. Abbas M (2020) Removal of brilliant green (BG) by activated carbon derived from medlar nucleus (ACMN)–Kinetic, isotherms and thermodynamic aspects of adsorption. Adsorption Science & Technology 38 (9-10):464-482

35. Mansour RAE-G, Simeda MG, Zaatout AA (2021) Removal of brilliant green dye from synthetic wastewater under batch mode using chemically activated date pit carbon. RSC Advances 11 (14):7851-7861

36. Kong L, Qiu F, Zhao Z, Zhang X, Zhang T, Pan J, Yang D (2016) Removal of brilliant green from aqueous solutions based on polyurethane foam adsorbent modified with coal. Journal of Cleaner Production 137 (1):51-59

37. Sarma G, Sen Gupta S, Bhattacharyya K (2019) Removal of hazardous basic dyes from aqueous solution by adsorption onto kaolinite and acid-treated kaolinite: kinetics, isotherm and mechanistic study. SN Applied Sciences 1 (3):1-15

38. Imran M, Islam AU, Tariq MA, Siddique MH, Shah NS, Khan ZUH, Amjad M, Din SU, Shah GM, Naeem MA (2019) Synthesis of magnetite-based nanocomposites for effective removal of brilliant green dye from wastewater. Environmental Science and Pollution Research 26 (24):24489-24502

39. Tanyol M, Kavak N, Torğut G (2019) Synthesis of poly (AN-co-VP)/zeolite composite and its application for the removal of brilliant green by adsorption process: kinetics, isotherms, and experimental design. Advances in Polymer Technology 2019 (1):1-12

40. Aichour A, Zaghouane-Boudiaf H (2019) Highly brilliant green removal from wastewater by mesoporous adsorbents: kinetics, thermodynamics and equilibrium isotherm studies. Microchemical Journal 146 (1):1255-1262